ISSN 1070-3632, Russian Journal of General Chemistry, 2021, Vol. 91, Suppl. 1, pp. S112–S122. © Pleiades Publishing, Ltd., 2021.

Some Novel [6-(Isoxazol-5-ylmethoxy)-3-methylbenzofuran-2-yl]phenylmethanone Derivatives, Their Antimicrobial Activity, and Molecular Docking Studies on COVID-19

N. Umapathi[a], B. Shankar[b], M. Raghavender[a], T. Vishnu[a], and P. Jalapathi[a,*]

[a] *Department of Chemistry, Osmania University, Hyderabad, Telangana, 500007 India*
[b] *School of Chemistry, University of Hyderabad, Central University, Telangana, 500046 India*
**e-mail: pochampalli.ou.chemi@gmail.com*

Received October 4, 2021; revised December 9, 2021; accepted January 23, 2022

Abstract—A novel series of benzofuran-isoxazole hybrid heterocyclic unit has been synthesized and their structures characterized by ^{1}H and ^{13}C NMR, and mass spectral data. The synthesized products have been evaluated for their *in vitro* antibacterial and antifungal activity using Gentamycin sulphate and Nystatin as standard drugs, respectively. Four synthesized products have been determined as highly active against all tested bacterial and fungal strains. Structure–antimicrobial activity relationship has been supported by docking studies of the active compounds against glucosamine-6-phosphate synthase and aspartic proteinase. According to the docking studies, all derivatives exhibit good theoretical affinity with Autodock 4.2 software score in the range of –9.37 and –11.63 kcal/mol against the main protease of COVID-19.

Keywords: benzofuran-isoxazole hybrids, antimicrobial activity, docking studies, COVID-19, Autodock 4.2

DOI: 10.1134/S1070363222020256

INTRODUCTION

Naturally occurring and synthetically prepared compounds containing 2-benzylbenzofuran moiety exhibit a wide range of pharmacological and biological activities [1]. Among those are antihyperglycemic [2], analgesic, antibacterial [3], anti-inflammatory [4], antifungal [5], and antitumor [6] agents. Attachment of other heterocyclic rings to benzofuran may lead to compounds of even higher activity against bacteria resistant to other drugs [7]. A number of natural and synthetic isoxazole based analogues such as ibotenic acid [8–10], muscimol [11] and some more exhibited valuable biological activities. Motivated by the above information on benzofuran and isoxazole derivatives, we have synthesized conjugated benzofuran-isoxazole derivatives targeting the potential pharmacophores.

RESULTS AND DISCUSSION

Synthetic approach to the new benzofuran-isoxazole hybrids **8a**–**8p** (Scheme 1) has not been presented in literature up to now.

Resorcinol (**1**) upon condensation with acetic acid in the presence of freshly fused $ZnCl_2$ led to 1-(2,4-dihydroxyphenyl)ethanone (**2**). The following selective *O*-alkylation of the semiproduct **2** by propargyl bromide in presence of K_2CO_3 afforded para alkylated compound **3** with 90% yield. 1-[2-Hydroxy-4-(prop-2-yn-1-yloxy)phenyl]ethanone (**3**) was subjected to condensation - cyclisation process with phenacyl bromide (**5**) in the presence of potassium carbonate with formation of [3-methyl-6-(prop-2-yn-1-yloxy)benzofuran-2-yl]-(phenyl)methanone (**6**) [12]. Some aliphatic and aromatic oxime intermediates **7a**–**7p** were synthesized according to the presented earlier methods [13]. Alkyl oximes were synthesized by heating their precursors, alkyl aldehyde, with hydroxyl amine hydrochloride in presence of sodium acetate in MeOH at room temperature. Aromatic oximes were prepared from different substituted benzaldehydes using sodium acetate. Finally, the *in situ* generated various substituted oximes **7a**–**7p** were subjected to 1,3-dipolar cycloaddition with terminal alkyne **6** in presence of copper sulphate to give the corresponding 3,5-disubstituted isoxazoles **8a**–**8p** [14].

Scheme 1. Synthesis of benzofuran-isoxazoles **8a**–**8p**.

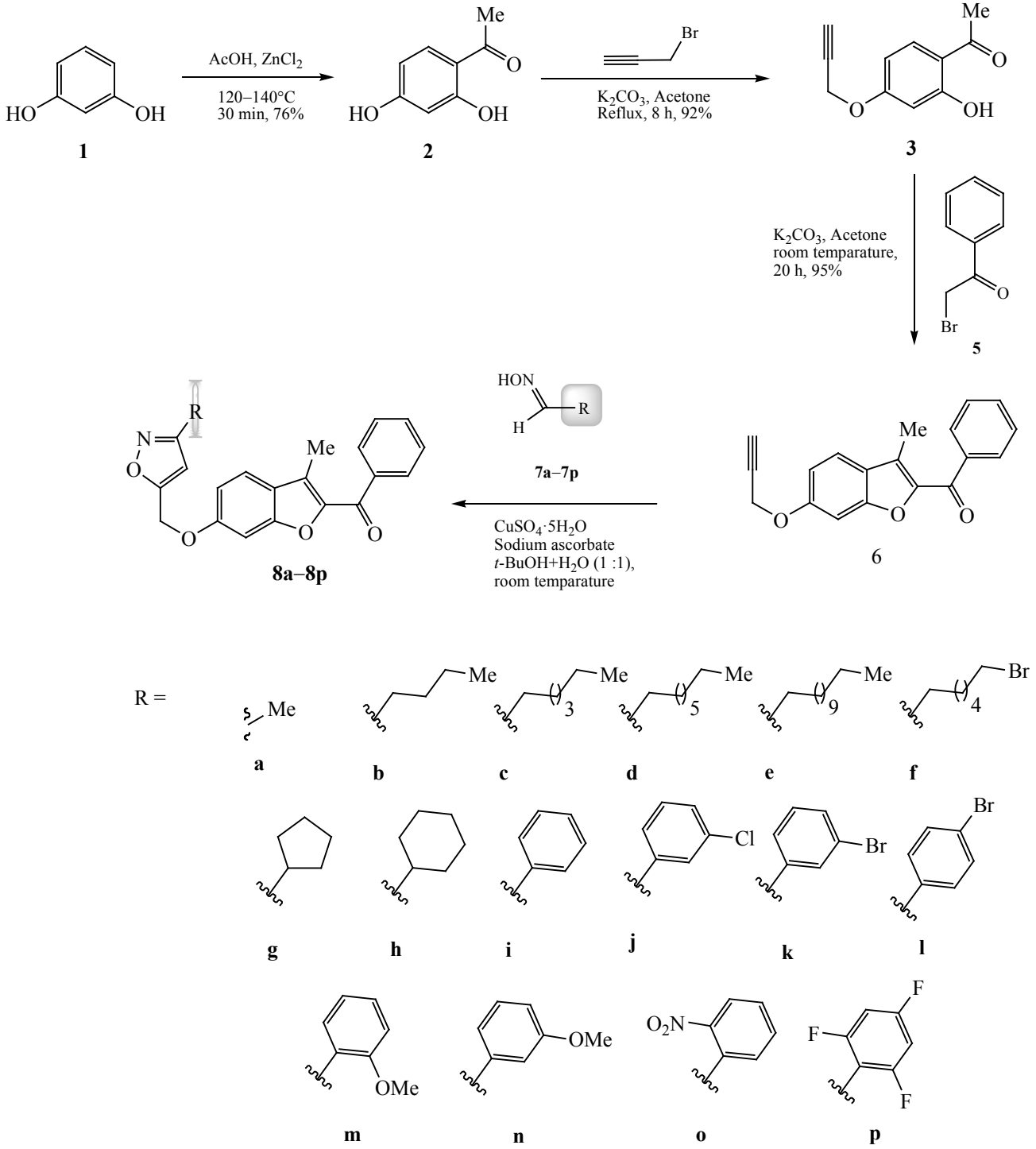

^{1}H and ^{13}C NMR, FTIR and mass spectral data were used to characterize structures of the newly synthesized target compounds.

Antibactericidal activity. Antibacterial tests of all synthesized products **8a**–**8p** exhibited activity (Table 1) on all species except *Salmonella typhi*. Compounds **8n**, **8j**, **8o**, **8i**, **8c**, and **8k** were determined to be highly active. The compounds with strong electron donating group like methoxy and weak electron withdrawing groups like fluoro and chloro on phenyl ring of oxazole enhanced

Table 1. Antibactericidal activity of the synthesized benzofuran based isoxazole analogues **8a**–**8p**

Tested compounds	Concentration (10^{-6} g/mL)	Inhibition zone (in 10^{-3} m)[a]									
		gram +ve bacteria					gram –ve bacteria				
		M. Tub	*M. lut*	*MRSA*	*B. sub*	*B. cer*	*P. aer*	*K. pne*	*E. col*	*P. vul*	*S. typ*
8a	75	20	20	20	19	20	16	20	20	18	06
	100	21	23	21	23	25	20	23	25	21	09
8b	75	20	16	22	19	NA	15	NA	20	17	NA
	100	23	15	25	21	NA	17	NA	28	19	NA
8c	75	20	22	23	23	24	22	21	26	23	NA
	100	22	25	25	27	29	28	24	29	27	NA
8d	75	17	15	14	14	13	13	13	16	15	NA
	100	19	17	19	17	23	18	19	22	19	NA
8e	75	17	19	13	12	13	12	14	15	14	NA
	100	18	19	17	15	19	17	18	22	18	NA
8f	75	20	19	18	13	15	17	14	20	13	NA
	100	23	22	23	17	26	19	18	28	24	NA
8g	75	23	23	22	20	21	16	20	20	21	NA
	100	25	25	26	27	28	20	24	28	24	NA
8h	75	14	17	21	16	20	16	16	20	18	NA
	100	25	23	27	18	25	18	20	23	21	NA
8i	75	24	23	26	24	23	22	22	26	24	NA
	100	29	23	27	28	32	28	28	32	28	NA
8j	75	28	23	25	23	26	22	23	28	24	NA
	100	33	25	31	31	32	29	28	32	28	NA
8k	75	21	24	23	22	24	20	20	23	21	NA
	100	23	26	24	25	28	23	23	28	25	NA
8l	75	17	15	16	10	12	11	14	16	14	NA
	100	17	14	17	14	17	15	18	19	17	NA
8m	75	22	21	23	21	24	21	21	23	20	NA
	100	25	23	28	26	28	24	25	28	24	NA
8n	75	28	26	27	27	32	28	28	33	29	NA
	100	31	27	30	30	33	29	26	31	32	NA
8m	75	28	24	26	26	28	25	23	28	25	NA
	100	29	27	31	30	31	27	27	31	29	NA
8p	75	17	16	17	14	22	16	20	19	18	NA
	100	20	21	25	21	25	25	25	23	25	NA
Zentamycin sulphate	75	29	27	31	30	31	28	27	31	29	NA
	100	32	30	33	33	34	31	30	33	31	NA

[a] (NA) No activity.

antibacterial activity in comparison with aliphatic aryl substituted oxazoles. However, strong electron withdrawing groups supported the activity as well. Compounds **8m**, **8g**, **8a**, **8h**, and **8f** also exhibited good antibacterial profile against the tested bacterial strains.

Antifungal activity. According to the results of tests presented in Table 2, the highest anti-fungal activity was determined for the products **8n**, **8j**, **8o**, **8i**, **8p**, and **8c** as compared with the standard Nystatin. *Trichophyton rubrum* and *Trichophyton interdigitale* exhibited resistance to all the products.

Table 2. Antifungal activity of the synthesized compounds **8a**–**8p**

Tested compounds	Concentration (10^{-6} g/mL)	Inhibition zone (in 10^{-3} m)[a]				
		M. canis	*M. gypseum*	*T. rubrum*	*T. interdigitale*	*E. floccosum*
8a	75	12	12	NA	NA	10
	100	15	15	NA	NA	16
8b	75	11	11	NA	NA	08
	100	14	14	NA	NA	12
8c	75	17	19	NA	NA	13
	100	21	24	NA	NA	18
8d	75	10	10	NA	NA	07
	100	14	16	NA	NA	11
8e	75	11	08	NA	NA	08
	100	13	13	NA	NA	09
8f	75	12	11	NA	NA	08
	100	14	14	NA	NA	13
8g	75	14	12	NA	NA	11
	100	17	16	NA	NA	16
8h	75	11	11	NA	NA	10
	100	15	15	NA	NA	12
8i	75	21	16	NA	NA	16
	100	23	20	NA	NA	17
8j	75	20	17	NA	NA	16
	100	26	22	NA	NA	18
8k	75	16	15	NA	NA	14
	100	21	19	NA	NA	18
8l	75	08	07	NA	NA	05
	100	12	09	NA	NA	08
8m	75	16	16	NA	NA	13
	100	18	18	NA	NA	15
8n	75	20	18	NA	NA	18
	100	28	21	NA	NA	20
8o	75	20	17	NA	NA	16
	100	22	19	NA	NA	19
8p	75	21	20	NA	NA	18
	100	23	24	NA	NA	16
Nystatin (std)	75	24	21	NA	NA	21
	100	27	25	NA	NA	24

[a] (NA) No activity.

Molecular Docking Studies

Antibacterial docking study. The compound **8m** and reference compound gentamycin were docked with Glucosamine-6-phosphate synthase (PDB ID: 2VF5). The Grid box was set up with 70 : 64 : 56 Å along *x*, *y*, and *z* points and coordinates 30.59, 15.822, and –3.497 were assigned to 2VF5 (Fig. 1) [15]. Both ligand and a molecule were loaded into ADT tool and saved in .pdbqt format. For obtaining best docking results 10 confirmers of ligand were run in Autodock 4.2. Docking score of the best conformer of compound **8m** was –9.29 kcal/mol whereas gentamycin score was –6.96 kcal/mole, and it demonstrated the higher value of binding energy than the reference compound with H-bond interactions with amino acid residues Thr302 and Ser303, and hydrophobic

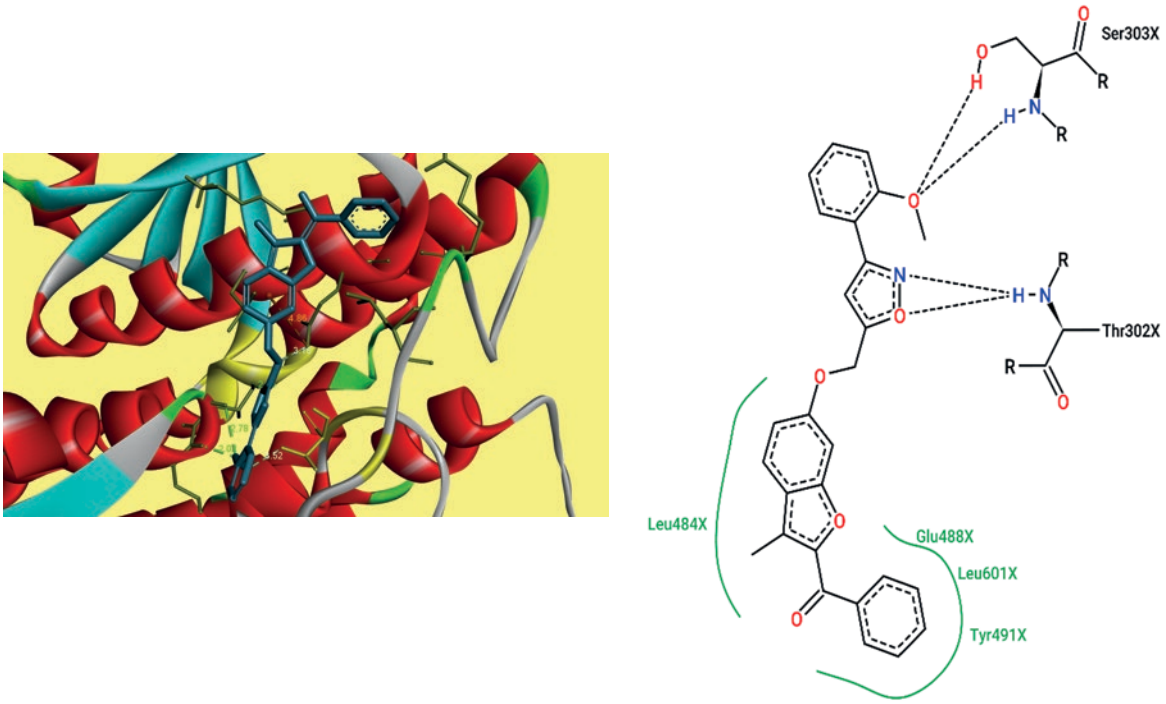

Fig. 1. Docking pose and 2D interactions of compound **8m** with 2VF5.

interactions with Leu484, Glu488, Tyr491, and Leu601 of 2VF5. Hence, the docking studies revealed that the newly synthesized compound **8m** was the efficient bacterial inhibitor.

Antifungal docking study. For estimating antifungal activity of compound **8n** and Nystatin these were docked into the active site of secreted aspartic proteinase (PDB ID: 2QZW). The ligand and proteins were loaded into ADT tool and saved in .pdbqt format. The Grid box for 2QZW (Fig. 2) was set up with 64 : 64 : 64 Å and coordinates –16.302, –23.24, and –16.245 were assigned [16]. The ligand was characterized by H-bond and hydrophobic interactions with the docking score of –10.03 kcal/mol on par with Nystatin whose score was –12.43 kcal/mol. The amino acid residues Asn131 and Arg192 of 2QZW were involved in H-bond interactions whereas Ile30, Ser35, Ile82, Tyr84, Gly85, Ile123, Ala335, and Asn337 were involved in hydrophobic interactions with the ligand **8n**. Hydrophobic interactions were not observed for Nystatin confirming the ligand **8n** to be the efficient antifungal agents.

Anti-Covid19 docking study. Docking simulations were carried out with each and every ligand on to the active site of COVID-19 main protease (PDB ID: 6LU7). After loading the ligands and protein those were saved in .pdbqt format. For 6LU7 (Fig. 3) the grid box was set up with 60 : 60 : 60 Å and coordinates –11.824, 14.735, and 74.152 were assigned [17]. Docking scores of the ligands were ranging from –9.37 to –11.63 kcal/mol. Binding energies of all the ligands are presented in Table 3. All the ligands were characterized by H-bond and hydrophobic interactions with 6LU7 except compound **8l**.

Compound **8j** demonstrated the highest docking score of –11.63 kcal/mol, and compounds **8k, 8n** and **8m** exhibited binding energies of –11.38, –10.94 and –10.91 kcal/mol, respectively. These compounds were characterized by H-bond and hydrophobic interactions with COVID-19 main protease at active site amino residues His41, Met49, Leu141, Gly143, Cys145, Met165, Glu166, Leu167, Pro168, Asp187, Arg188, and Gln189. These results revealed that the ligands were potent inhibitors of COVID-19 main protease.

EXPERIMENTAL

Melting points were measured in open capillaries and are uncorrected. TLC was carried out on silica gel-G, and the spots were visualized under UV light at 254 nm. Column chromatography was performed on a Merck silica

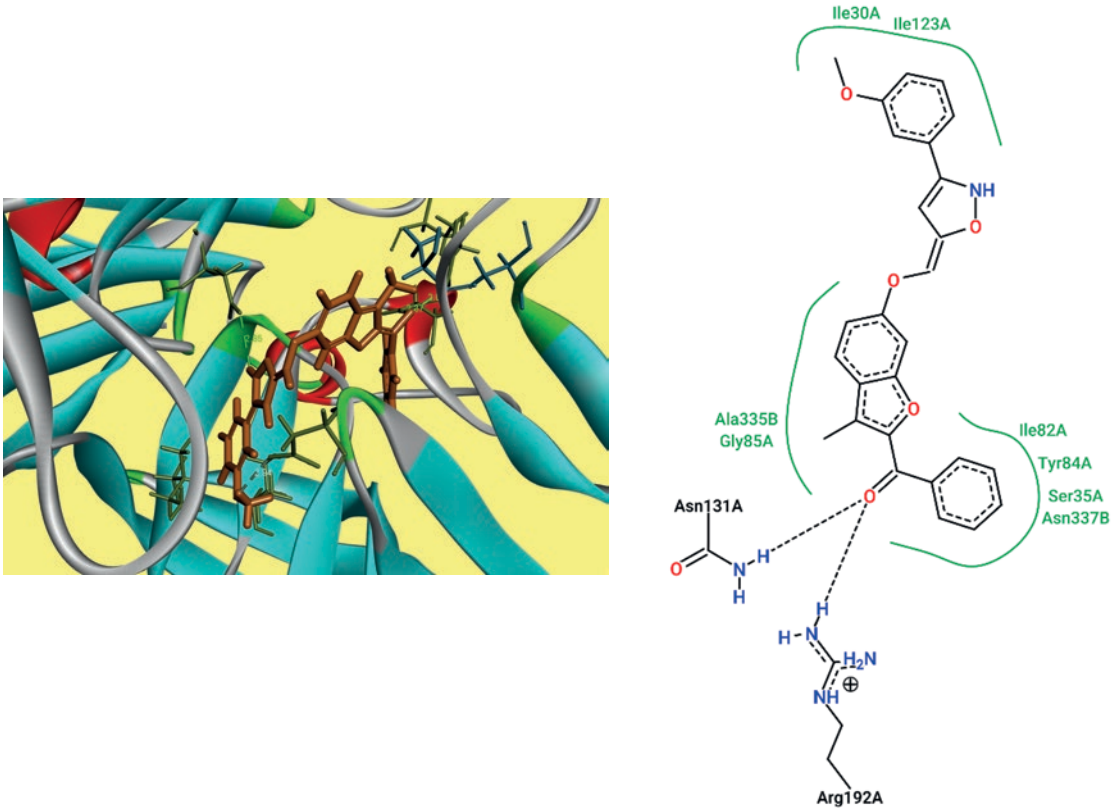

Fig. 2. Docking pose and 2D interactions of compound **8n** with 2QZW.

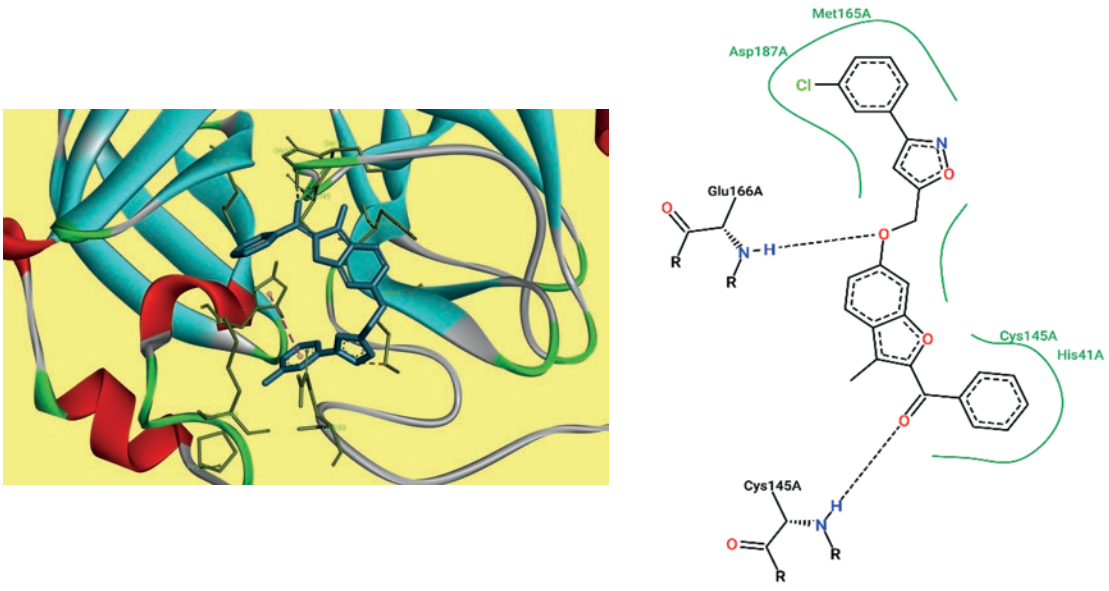

Fig. 3. Docking pose and 2D interactions of compound **8j** with 6LU7.

gel 60A (100–200 mesh). IR spectra (KBr discs) were recorded on a Perkin-Elmer 1000 spectrophotometer. NMR spectra were measured on a Bruker AV-400 and AV-300 spectrometers using $CDCl_3$ as a solvent and TMS as an internal standard. Mass spectra were measured on an Agilent LC-MS instrument.

Table 3. Docking scores of the compounds **8a**–**8p** with COVID-19 main protease (PDB ID: 6LU7)

Compound	Binding score, kcal/mol	Interacting amino acid residues
8a	–9.37	Thr25, Cys145, His163
8b	–10.45	Phe140, Leu141, Gly143, Glu166, Arg188
8c	–9.68	Met49, His41, Leu141, Gly143, Cys145, Met165
8d	–9.83	Thr25, Cys145, Met165, Glu166, Arg188
8e	–9.82	Met165, Glu166, Gln189
8f	–10.69	His41, Gly143, Cys145, Met165, Asp187
8g	–10.59	His41, Met49, Leu141, Gly143, Cys145, Met165
8h	–10.95	His41, Met49, Leu141, Gly143, Cys145, Met165, Leu167, Pro168, Gln192
8i	–10.73	Thr25, Leu27, His41, Ser144, Cys145, Met165, Asp187
8j	–11.63	His41, Cys145, Met165, Glu166, Asp187
8k	–11.38	His41, Met49, Leu141, Gly143, Cys145, Met165, Leu167
8l	–10.97	No interactions
8m	–10.91	His41, Met49, Gly143, Cys145, Met165, Glu166, Asp187, Arg188, Gln189
8n	–10.94	His41, Leu141, Gly143, Cys145, Met165, Leu167, Pro168
8o	–11.29	Thr25, Leu27, His41, Met49, Gly143, Ser144, Cys145, Met165, Asp187, Gln189
8p	–10.62	His41, Met49, Leu141, Gly143, His163, Met165

Synthesis of 1-(2,4-dihydroxyphenyl) ethanone (2). A mixture of freshly fused $ZnCl_2$ (6.8 g, 0.05mol) with acetic acid (3 g, 0.05mol) was boiled at 120°C for 30 min, then resorcinol (**1**) (5.5 g, 0.05mol) was added to it. The mixture was boiled for 30 min at 140°C upon monitoring of the process by TLC. The mixture was cooled down to room temperature, mixed with cold H_2O (100 mL) and extracted with ethyl acetate (3×50 mL). The mixture of organic layers was washed by 20% hydrochloric acid (50 mL), saturated $NaHCO_3$ (25 mL) and brine solution (2×25 mL) then dried by anhydrous sodium sulphate, filtered and concentrated under vacuum. The crude product was purified by column chromatography with silica gel 100–200 mesh using 10% $CH_3COOC_2H_5$–hexane. The pure product **2** was isolated in the form of reddish brown needles.

Synthesis of 1-[2-hydroxy-4-(prop-2-yn-1-yloxy)-phenyl]ethanone (3). Propargyl bromide was added dropwise to a well agitated solution of 1-(2,4-dihydroxy-phenyl) ethanone (**2**) (3.0 g, 0.019 mol) in dry acetone and K_2CO_3 (2.72 g, 0.019 mol) followed by refluxing the mixture for 8 h (TLC). The mixture was cooled down to room temperature, and acetone was evaporated under reduced pressure. The residue was extracted with water (50 mL) and ethyl acetate (3×50 mL). The mixture of organic layers was washed with salt solution (2× 25 mL). Organic layer was dried over anhydrous Na_2SO_4, then filtered and concentrated under vacuum. The crude product was purified by column chromatography using 5% ethyl acetate in hexane to obtain compound **3** as white solid.

Synthesis of [3-methyl-6-(prop-2-yn-1-yloxy) benzo-furan-2-yl]phenylmethanone (6). A mixture of (2 g, 0.010 mol) phenacylbromide (**5**) with compound **3** (2.09 g, 0.010 mol) and K_2CO_3 (2.90 g, 0.02mol) was heated in acetone (20 mL) for 20 h [12] (TLC). The residue was filtered off and washed with acetone (2 × 15 mL), then it was purified by column chromatography using 10% ethyl acetate in petroleum ether as an eluent, yield 95%.

General procedure for the synthesis of oxime mediates 7a–7p. To the aldehyde (1 eq.) solution in methanol were added hydroxylamine hydrochloride (1 eq.) followed by sodium acetate (1.5 eq.). The mixture was agitated for ca 3 h (TLC). Upon completion of the reaction, the mixture was quenched by ice. The resulting precipiate was filtered and extracted, then washed by hexane and dried.

General procedure for the synthesis of isoxazoles 8a–8p. The intermediate **5** (200 mg, 0.375 mmol) was dissolved in 10 mL of aqueous t-BuOH (50%) and mixed with $CuSO_4 \cdot 5H_2O$ (5 mol %), sodium ascorbate (10 mol %) and a desired oxime **7a**–**7p** (0.45 mmol). The reaction mixture was stirred for 1 h at room temperature (TLC). Upon completion of the process, the reaction mixture was diluted with H_2O (25 mL) and extracted with C_2H_5OAc

(3×25 mL). The combined organic layers were washed with brine (2×25 mL), dried over anhydrous sodium sulphate, filtered, and concentrated in vacuum. The crude product was purified by column chromatography using ethyl acetate in hexane as an eluent to afford the corresponding product **8a**–**8p**.

{3-Methyl-6-[(3-methylisoxazol-5-yl)methoxy}-benzofuran-2-yl}phenylmethanone (8a). Yellow solid, yield 70%, mp 167–169°C. IR spectrum, ν, cm^{-1}: 1646 (C=O), 1560, 1250, 1100. ^{1}H NMR spectrum, δ, ppm: 8.14–7.99 m (2H), 7.69–7.44 m (5H), 7.14 s (1H), 7.07–6.95 m (1H), 5.27 s (2H), 4.37 t (2H, *J* = 6.47 Hz), 2.60 s (3H), 1.98–1.82 m (2H), 1.43–1.30 m (2H), 1.03–0.87 m (3H). ^{13}C NMR spectrum, δ, ppm: 185.3, 159.6, 155.5, 148.3, 143.5, 138.0, 132.3, 129.6 (2C), 128.2 (2C), 127.6, 123.1, 122.6, 121.9, 114.0, 96.7, 62.5, 50.4, 31.0, 30.1, 22.4, 10.2. MS: *m/z*: 390.2 $[M + H]^+$.

{3-Methyl-6-[(3-methylisoxazol-5-yl)methoxy]-benzofuran-2yl}phenylmethanone (8b). White solid, yield 93%, mp 196–198°C. IR spectrum, ν, cm^{-1}: 1720 (C=O), 1545, 1260, 1015, 980. ^{1}H NMR spectrum, δ, ppm: 8.08 d (2H, *J* = 7.42 Hz), 7.66–7.51 m (5H), 7.16 d (1H, *J* = 1.72 Hz), 7.06–7.02 m (1H), 5.30 s (2H), 4.37 t (2H, *J* = 7.27 Hz,), 2.62 s (3H), 1.98–1.88 m (2H), 1.31 d (6H, *J* = 10.93 Hz,), 0.88 t (3H, *J* = 6.86 Hz). ^{13}C NMR spectrum, δ, ppm: 185.3, 159.6, 155.5, 148.3, 143.5, 138.1, 132.3, 129.6 (2C), 128.2 (2C), 127.5, 123.2, 122.5, 121.9, 114.0, 96. MS: *m/z*: 348.1 $[M + H]^+$.

{6-[(3-Hexylisoxazol-5-yl)methoxy]-3-methyl-benzofuran-2-yl}phenylmethanone (8c). White solid, yield 93%, mp 103–105°C. IR spectrum, ν, cm^{-1}:1720 (C=O), 1635, 1452, 1250, 1150. ^{1}H NMR spectrum, δ, ppm: 8.08 d (2H, *J* = 7.42 Hz), 7.66–7.51 m (5H), 7.16 d (1H, *J* = 1.72 Hz), 7.06–7.02 m (1H), 5.30 s (2H), 4.37 t (2H, *J* = 7.27 Hz), 2.62 s (3H), 1.98–1.88 m (2H), 1.31 d (6H, *J* = 10.93 Hz), 0.88 t (3H, *J* = 6.86 Hz). ^{13}C NMR spectrum, δ, ppm: 185.3, 159.6, 155.5, 148.3, 143.5, 138.1, 132.3, 129.6, 128.2, 127.5, 123.2, 122.5, 121.9, 114.0, 96.8, 62.6, 50.5, 31.1, 30.2, 26.1, 22.3, 13.9, 10.1. MS: *m/z*: 418 $[M + H]^+$.

{3-Methyl-6-[(3-octylisoxazol-5-yl)methoxy]benzo-furan-2-yl}phenylmethanone (8d). Yellow solid, yield 94%, mp 165–167°C. IR spectrum, ν, cm^{-1}: 1760 (C=O), 1645, 1287, 1150, 960. ^{1}H NMR spectrum, δ, ppm: 8.06 d (2H , *J* = 6.72 Hz), 7.69–7.44 m (5H), 7.14 s (1H), 7.03 d (1H, *J* = 7.90 Hz), 5.28 s (2H), 4.36 t (2H, *J* = 6.47 Hz), 2.61 s (3H), 1.99–1.82 m (2H), 1.38–1.17 m (10H), 0.94–0.79 m (3H). ^{13}C NMR spectrum, δ, ppm: 185.3, 159.6, 155.5, 148.3, 143.5, 138.0, 132.3, 129.6, 128.3, 127.6, 123.1, 122.6, 121.9, 114.0, 96.7, 62.5, 50.5, 31.7, 30.2, 29.0, 28.9, 26.5, 22.6, 14.0, 10.2. MS: *m/z*: 446.5 $[M + H]^+$.

{6-[(3-Dodecylisoxazol-5-yl)methoxy]-3-methyl-benzofuran-2-yl}phenylmethanone (8e). White solid, yield 94%, mp 169–171°C. IR spectrum, ν, cm^{-1}: 1646 (C=O), 1620, 1263, 1075. ^{1}H NMR spectrum, δ, ppm: 8.08 d (2H, *J* = 7.68 Hz), 7.65 s (1H), 7.63–7.49 m (4H), 7.16 s (1H), 7.04 d (1H, *J* = 8.66 Hz), 5.29 s (2H), 4.37 t (2H, *J* = 7.19 Hz), 2.62 s (3H), 2.03–1.84 m (2H), 1.38–1.24 m (18H), 0.89 t (3H, *J* = 6.56 Hz). ^{13}C NMR spectrum, δ, ppm: 185.3, 159.6, 155.5, 148.3, 143.5, 138.0, 132.3, 129.5, 128.2, 127.6, 123.0, 122.6, 121.9, 114.0, 96.6, 62.5, 51.1, 33.7, 32.2, 30.6, 28.9, 26.9, 26.5, 24.5, 22.6, 20.2, 17.3, 14.0, 10.2. MS: *m/z*: 502.4 $[M + H]^+$.

(6-{[3-(6-Bromohexyl)isoxazol-5-yl]methoxy}-3-methylbenzofuran-2-yl)phenylmethanone (8f). Yellow solid, yield 73%, mp 168–170°C. IR spectrum, ν, cm^{-1}: 1754, 1612, 1478, 1150, 980. ^{1}H NMR spectrum, δ, ppm: 8.06 d (2H, *J* = 7.10 Hz), 7.67–7.49 m (5H), 7.14 s (1H), 7.07–6.99 m (1H), 5.28 s (2H), 4.38 t (2H, *J* = 6.36 Hz), 3.38 t (2H, *J* = 6.06 Hz), 2.61 s (3H), 1.98–1.77 m (4H), 1.49–1.28 m (4H). ^{13}C NMR spectrum, δ, ppm: 185.3, 159.5, 155.4, 148.2, 143.5, 138.0, 132.3, 129.5, 128.2, 127.5, 123.1, 122.6, 121.9, 114.0, 96.6, 62.5, 50.2, 33.5, 32.3, 30.0, 27.4, 25.6, 10.2. MS: *m/z*: 496.2 $[M + H]^+$.

{6-[(3-Cyclopentylisoxazol-5-yl)methoxy]-3-methylbenzofuran-2-yl-phenylmethanone (8g). White solid, yield 85%, mp 168–170°C. IR spectrum, ν, cm^{-1}: 1647 (C=O), 1450, 1230, 1122, 1015, 860. ^{1}H NMR spectrum, δ, ppm: 8.06 d (2H, *J* = 7.29 Hz), 7.70 s (1H), 7.64–7.48 m (4H), 7.15 s (1H), 7.03 d.d (1H, *J* = 8.65, 1.70 Hz), 5.26 s (2H), 4.99-4.89 m (1H), 2.63 s (3H), 2.32–2.21 m (2H), 2.12–2.01 m (2H), 1.97–1.86 m (2H), 1.82–1.70 m (2H). ^{13}C NMR spectrum, δ, ppm: 185.3, 159.7, 155.5, 148.3, 143.2, 138.0, 132.3, 129.6, 128.2, 127.5, 123.1, 121.9, 121.3, 114.0, 96.7, 62.6, 62.0, 33.3, 24.0, 10.1. MS: *m/z*: 402.3 $[M + H]^+$.

{6-[(3-Cyclohexylisoxazol-5-yl)methoxy]-3-methylbenzofuran-2-yl}phenylmethanone (8h). Pale yellow solid, yield 81%, mp 157–159°C. IR spectrum, ν, cm^{-1}: 1670 (C=O), 1600, 1450, 1240, 630. ^{1}H NMR spectrum, δ, ppm: 8.05 d (2H, *J* = 6.40 Hz), 7.65 s (1H), 7.61–7.42 m (4H), 7.13 s (1H), 7.01 d (1H, *J* = 7.75 Hz), 5.24 s (2H), 4.43 s (1H), 2.58 s (3H), 2.20 d (2H, *J* = 9.62 Hz), 1.90 d (2H, *J* = 11.15 Hz), 1.73 d (3H, *J* = 10.99 Hz), 1.43 d (2H, *J* = 12.43 Hz), 1.25 d (1H, *J* =

11.51 Hz). ^{13}C NMR spectrum, δ, ppm: 185.3, 159.7, 155.5, 148.2, 142.9, 138.0, 132.3, 129.5, 128.2, 127.6, 123.0, 121.9, 120.6, 114.0, 96.5, 62.5, 60.2, 33.5, 25.1, 25.0, 10.2. MS: *m/z*: 416.5 $[M + H]^+$.

{3-Methyl-6-[(3-phenylisoxazol-5-yl)methoxy]-benzofuran-2-yl}phenylmethanone (8i). White solid, yield 88%, mp 127–130°C. IR spectrum, ν, cm^{-1}: 1720 (C=O), 1650, 1578, 1240, 1100, 680. ^{1}H NMR spectrum, δ, ppm: 8.12–8.07 m (3H), 7.77–7.75 m (2H), 7.62–7.59 m (2H), 7.57–7.52 m (4H), 7.48–7.45 m (1H), 7.20 d (1H, *J* = 2.12 Hz), 7.08 d.d (1H, *J* = 8.69, 2.20 Hz), 5.39 s (2H), 2.63 s (3H). ^{13}C NMR spectrum, δ, ppm: 185.3, 159.5, 155.5, 148.4, 144.4, 138.0, 136.9, 132.3, 129.8, 129.6, 128.9, 128.2, 127.5, 123.3, 122.0, 121.0, 120.6, 114.0, 96.9, 62.5, 10.1. MS: *m/z*: 410.4 $[M + H]^+$.

(6-{[3-(3-Chlorophenyl)isoxazol-5-yl]methoxy}-3-methylbenzofuran-2-yl)phenylmethanone (8j). Pale yellow solid, yield 78%, mp 168–170°C. IR spectrum, ν, cm^{-1}: 1664, 1498, 1232, 1100, 1098, 680. ^{1}H NMR spectrum, δ, ppm: 8.15–7.99 m (3H), 7.77 s (1H), 7.67–7.37 m (7H), 7.14 s (1H), 7.03 d (1H, *J* = 8.28 Hz), 5.33 s (2H), 2.59 s (3H). ^{13}C NMR spectrum, δ, ppm: 185.3, 159.4, 155.4, 148.3, 137.9, 137.6, 135.6, 132.4, 130.8, 129.6, 129.5, 129.0, 128.2, 127.5, 123.2, 122.0, 121.0, 120.7, 118.4, 113.9, 96.6, 62.2, 10.2. MS: *m/z*: 444 $[M + H]^+$.

(6-{[3-(3-Bromophenyl)isoxazol-5-yl]methoxy}-3-methylbenzofuran-2-yl)phenylmethanone (8k). Light yellow solid, yield 81%, mp 154–156°C. IR spectrum, ν, cm^{-1}: 1663 (C=O), 1600, 1548, 1230, 1100, 1005, 980, 750. ^{1}H NMR spectrum, δ, ppm: 8.11 s (1H), 8.07 d (2H, *J* = 7.16 Hz), 7.66–7.43 m (8H), 7.19 d (1H, *J* = 2.01 Hz), 7.07 d.d (1H, *J* = 8.69, 2.11 Hz), 5.38 s (2H), 2.61 s (3H). ^{13}C NMR spectrum, δ, ppm: 185.4, 159.6, 155.5, 148.3, 143.4, 138.0, 134.7, 132.4, 130.9, 130.8, 129.6, 128.5, 128.3, 128.0, 127.8, 127.6, 125.0, 123.3, 122.0, 114.1, 96.8, 62.4, 10.2. MS: *m/z*: 444.2 $[M + H]^+$.

(6-{[3-(4-Bromophenyl)isoxazol-5-yl]methoxy}-3-methylbenzofuran-2-yl)phenylmethanone (8l). Brick red solid, yield 91%, mp 138–140°C. IR spectrum, ν, cm^{-1}: 1666 (C=O), 1546, 1456, 1234, 1100, 1005, 965, 650. ^{1}H NMR spectrum, δ, ppm: 8.13–8.04 m (3H), 7.70 d (2H, *J* = 8.81 Hz), 7.63–7.57 m (2H), 7.56–7.48 m (4H), 7.17 d (1H, *J* = 1.99 Hz), 7.07–7.03 m (1H), 5.38 s (2H), 2.61 s (3H). ^{13}C NMR spectrum, δ, ppm: 185.3, 159.5, 155.5, 148.3, 144.6, 138.0, 135.4, 134.8, 132.4, 130.0, 129.6, 128.3, 127.5, 123.3, 122.0, 121.7, 121.0, 113.9, 96.8, 62.4, 10.2. MS: *m/z*: 444.2 $[M + H]^+$.

(6-{[3-(2-Methoxyphenyl)isoxazol-5-yl]methoxy}-3-methylbenzofuran-2-yl)phenylmethanone (8m). White solid, yield 86%, mp 168–170°C. IR spectrum, ν, cm^{-1}: 1750 (C=O), 1600, 1554, 1420, 1230, 1100, 630. ^{1}H NMR spectrum, δ, ppm: 8.23 s (1H), 8.11–8.04 m (2H), 7.80 d.d (1H, *J* = 7.88,1.54 Hz), 7.64–7.49 m (4H), 7.47–7.40 m (1H), 7.20 d (1H, *J* = 2.04 Hz), 7.15–7.04 m (3H), 5.37 s (2H), 3.88 s (3H), 2.62 s (3H). ^{13}C NMR spectrum, δ, ppm: 185.4, 159.7, 155.5, 151.0, 148.3, 142.8, 138.0, 132.3, 130.2, 129.6, 128.3, 127.6, 126.1, 125.5, 125.2, 123.2, 121.9, 121.2, 114.2, 112.2, 96.8, 62.5, 56.0, 10.2. MS: *m/z*: 440.4 $[M + H]^+$.

(6-{[3-(3-methoxyphenyl)isoxazol-5-yl]methoxy}-3-methylbenzofuran-2-yl)phenylmethanone (8n). Brick red solid, yield 87%, mp 136–138°C. IR spectrum, ν, cm^{-1}: 1650 (C=O), 1540, 1250, 1003, 630. ^{1}H NMR spectrum, δ, ppm: 8.41 d (2H, *J* = 8.84 Hz), 8.22 s (1H), 8.08–7.95 m (4H), 7.62–7.56 m (2H), 7.54–7.48 m (2H), 7.16 s (1H), 7.05 d (1H, *J* = 8.60 Hz), 5.38 s (2H), 2.59 s (3H). ^{13}C NMR spectrum, δ, ppm: 185.3, 159.2, 155.4, 148.3, 147.3, 145.3, 140.9, 137.9, 132.4, 129.5, 128.2, 127.4, 125.5, 123.4, 122.1, 120.8, 120.5, 113.8, 96.7, 62.2, 10.1. MS: *m/z*: 455.0 $[M + H]^+$.

(3-Methyl-6-{[3-(2-nitrophenyl)isoxazol-5-yl]-methoxy}benzofuran-2-yl)phenylmethanone (8o). Yellow solid, yield, 91%, mp 148–150°C. IR spectrum, ν, cm^{-1}: 1680 (C=O), 1520, 1423, 1122, 1010, 890. ^{1}H NMR spectrum, δ, ppm: 8.59 s (1H), 8.32–8.23 m (2H), 8.22–8.13 m (1H), 8.04 d (2H, *J* = 7.43 Hz), 7.73 t (1H, *J* = 8.15 Hz), 7.62–7.45 m (4H), 7.14 s (1H), 7.03 d (1H, *J* = 8.29 Hz), 5.36 s (2H), 2.57 s (3H). ^{13}C NMR spectrum, δ, ppm: 185.3, 159.3, 155.4, 148.8, 148.3, 145.1, 137.9, 137.5, 132.4, 131.0, 129.5, 128.2, 127.5, 125.9, 123.3, 123.3, 122.1, 121.0, 115.2, 113.9, 96.6, 62.2, 10.2. MS: *m/z*: 455.2 $[M + H]^+$.

(3-Methyl-6-{[3-(2,4,6-trifluorophenyl)isoxazol-5-yl]methoxy}benzofuran-2-yl)phenylmethanone (8p). White solid, yield 85%, mp 149–147°C. IR spectrum, ν, cm^{-1}: 1770 (C=O), 1650, 1432, 1012, 960. ^{1}H NMR spectrum, δ, ppm: 8.17 d (1H, *J* = 2.72 Hz), 8.10–8.03 m (2H), 7.78–7.69 m (1H), 7.63–7.48 m (4H), 7.24–7.14 m (2H), 7.06 d.d (1H, *J* = 8.69, 2.15 Hz), 5.37 s (2H), 2.61 s (3H). ^{13}C NMR spectrum, δ, ppm: 185.3, 159.4, 155.4, 148.3, 144.5, 139.3, 138.0, 132.4, 129.6, 128.3, 127.5, 123.9, 123.3, 122.6, 122.1, 118.8, 114.01, 113.0, 96.8, 62.2, 10.2. MS: *m/z*: 464.3 $[M + H]^+$.

Anti-microbial assay. Solution of a tested compound (1 mg/mL) in DMSO was impregnated on sterilized

standard discs of filter paper (5 mm). The discs soaked with the test compound were placed on an agar plate injected with test organism. The tests were carried out in triplicates. The zentamycin sulphate and nystatin were used as the standards. All the petri plates were incubated at 37°C for one to five days. The results were estimated by measuring the diameter of inhibition zones (Tables 1 and 2). The most active compounds were further subjected to determination of their minimum inhibitory concentrations (MICs).

Minimal inhibition concentration (MIC) measurement. To determine the MIC vulnerability tests of microorganism in nutrient and dextrose broths were employed. DMSO (1000 μg/mL) was used to prepare stock solutions of Ciproflaxin (standard antibacterial agent), Nystatin (standard antifungal agent) and test compounds. The following dilutions of the above solutions gave concentrations ranging from 25 to 250 μg/mL. The suspensions of microbial cultures were inoculated on to agar plates and then discs of test and control compounds of different concentrations were placed on agar surface (Tables 1 and 2).

Docking procedure. The open source software Autodock 4.2 was downloaded from the Scripps Research Institute (www.scripps.edu) into the computer configured with Intel(R) Core(TM) i5-8250U CPU @ 1.60GHz 1.80 GHz processor and RAM capacity of 8.00GB. The ligand molecules were drawn using the tool ChemSketch (www.acdlabs.com) in .mol format and converted to PDB file using Pymol (pymol.org) program tool.

To study the binding interactions between the newly synthesized ligands and the target molecules, glucosamine 6-phosphate synthase from Escherichia Coli (PDB ID: 2VF5), the Secreted aspartic proteinase from Candida albicans (PDB ID: 2QZW) and Covid-19 main protease (PDB ID: 6LU7) were downloaded from Protein Data Bank (www.rcsb.org). The ligands and the target proteins were loaded into Autodock 4.2, the number of torsions were set to the ligands. Both ligand and target proteins were saved into .pdbqt format. The Grid box and x, y, z centres were assigned to the active site of proteins.

The Autodock 4.2 uses a Lamarckian genetic algorithm program to calculate different ligand conformers. Conformations were ranked according to the binding energy obtained from docked procedure and the confirmation with lowest binding energy was considered as the best docking score. The Autodock 4.2 results were visualized by using BIOVIA Discovery Studio Visualizer and Proteins Plus Server (https://proteins.plus/).

CONCLUSIONS

A new class of benzofuran-isoxazoles (**8a**–**8p**) has been successfully synthesized in high yields and characterized by spectroscopic methods. All newly synthesized compounds have demonstrated high antibacterial and antifungal activities. The compounds **8m**, **8n**, **8j**, and **8k** have been determined to be the most active. Molecular docking studies have been performed for all compounds into the binding cavity of protein 2VF5, 2QZW, and 6LU7. Docking scores of the best conformers of compounds are as follows: –9.29 kcal/mol for **8m** against 2VF5, –10.03 kcal/mol for **8n** against 2QZW, and –11.63 kcal/mol for **8j** against 6LU7. All products have demonstrated docking scores ranging from –9.37 to –11.63 kcal/mol with COVID-19 Main Protease. Hence, all newly synthesized benzofuran-isoxazoles ligands need further studies as the potential therapeutic agents for COVID-19.

AUTHOR INFORMATION

N. Umapathi, ORCID: https://orcid.org/0000-0002-2178-1999

B. Shankar, ORCID: https://orcid.org/0000-0001-5414-3662

M. Raghavendera, ORCID: https://orcid.org/0000-0001-7354-4568

T. Vishnua, ORCID: https://orcid.org/0000-0001-6830-3671

P. Jalapathi, ORCID: https://orcid.org/0000-0002-5419-6868

ACKNOWLEDGMENTS

N. Umapathi thanks the Head of the Department, Osmania University, Hyderabad, India and Research and Development central facilities, Osmania University, Hyderabad, India for providing analytical support. B.S. thanks the University Grants Commission in India for the award of a Dr. D. S. Kothari postdoctoral fellowship.

CONFLICT OF INTEREST

No conflict of interest was declared by the authors.

REFERENCES

1. Rawat, P., Kumar, M., Rahuja, N., Srivastava, D.S.L., Srivastava, A.K., and Maurya, R., *Bioorg. Med. Chem. Lett.*, 2011, vol. 21, p. 228. https://doi.org/10.1016/j.bmcl.2010.11.031Get
2. Cottineau, B., Toto, P., Marot, C., Pipaud, A., and Chenault, J., *Bioorg. Med. Chem. Lett.*, 2002, vol. 12, p. 2105. https://doi.org/10.1016/S0960-894X(02)00380-3
3. Manna, K. and Agrawal, Y.K., *Bioorg. Med. Chem. Lett.*, 2009, vol. 19, p. 2688. https://doi.org/10.1016/j.bmcl.2009.03.161
4. Chakrabarti, J.K., Eggleton, R.J., Gallagher, P.T., Harvey, J., Hicks, T.A., Kitchen, E.A., and Smith, C.W., *J. Med. Chem.*, 1987, vol. 30, p. 1663. https://doi.org/10.1021/jm00392a024
5. Gündoğdu-Karaburun, N., Benkli, K., Tunali, Y., Uçucu, Ü., and Demirayak, Ş., *Eur. J. Med. Chem.*, 2006, vol. 41, p. 651. https://doi.org/10.1016/j.ejmech.2005.12.013
6. Galal, S.A., El-All, A.S.A., Abdallah, M.M., and El-Diwani, H.I., *Bioorg. Med. Chem. Lett.*, 2009, vol. 19, p. 2420. https://doi.org/10.1016/j.bmcl.2009.03.069
7. Kumbhare Ravindra, M., *Bioorg. Med. Chem. Lett.*, 2012, vol. 22(17) p. 5424. https://doi.org/10.1016/j.bmcl.2012.07.041
8. Naeimi, H., Amini, A., and Moradian, M., *Org. Chem. Front*., 2014, vol. 1, p. 415. https://doi.org/10.1039/C4QO00031E
9. Naeimi, H. and Moradi, L., *Catal. Commun.*, 2006, vol. 7, p. 1067. https://doi.org/10.1016/j.catcom.2006.04.012
10. Sharghi, H., Hosseini-Sarvari, M., and Eskandari, R., *Synthesis*, 2006, p. 2047.
11. Kumar, S., Reddy, L., Shekhar, C., Kumar, Y., Kumar, A., Singh, B.K., Kumar, V., Malhotra, S., Pandey, M.K., and Jain, R., *Arch. Pharm*., 2012, vol. 345, p. 368. https://doi.org/10.1002/ardp.201100279
12. Shankar, B., Jalapathi, P., Ramesh, M., Kishore Kumar, A., Ragavender, M., and Bharath, G., *Russ. J. Gen. Chem.*, 2016, vol. 86, p. 1711. https://doi.org/10.1134/S107036321607029X
13. Sharghi, H. and Hosseini-Sarvari, R.M., and Eskandari, *Synthesis*, 2006, p. 2047.
14. Hansen, T.V., Wu, P., and Fokin, V.V., *J. Org. Chem*., 2005, vol. 70, p. 7761. https://doi.org/10.1021/jo050163b
15. Akansha, A., Rajesh Kumar, P., and Virendra, K., *Arab. J. Sci. Eng.*, 2022, vol. 47, p. 347. https://doi.org/10.1007/s13369-021-05377-1
16. Abhishek, B., Venkataraghavan, R., Vivek, P., and Ivo Romauld, S., *J. App. Pharm. Sci.*, 2019, vol. 9, p. 021. https://doi.org/10.7324/JAPS.2019.90503
17. Nagamani, M., Vishnu, T., Jalapathi, P., and Srinivas, M., *J. Iran. Chem. Soc.*, 2021. https://doi.org/10.1007/s13738-021-02365-y